Speed Control of PMBLDC Motor Using Rotor Position Rotor Speed PWM Technique

Rajen Pudur and Brajagopal Datta

Nomenclature

A	Area (m^2)
a	Length of specimen (m)
D	Diameter of rod (m)

Greek Symbols

α	Volume fraction (dimensionless)
η	Efficiency (dimensionless)

Superscripts

(n)	nth iteration

Subscripts

a	Air

R. Pudur · B. Datta (✉)
Department of Electrical Engineering, NIT Arunachal Pradesh, Yupia, India
e-mail: brajagopal@nitap.ac.in

P. Mahanta et al. (eds.), *Advances in Thermofluids and Renewable Energy*, Lecture Notes in Mechanical Engineering, https://doi.org/10.1007/978-981-16-3497-0_49

1 Introduction

Recent technology advancement in DC motors for electric bike resulted in new energy efficient derives using PMBLDC motors. A BLDC motor has windings on stator and alternate permanent magnets on rotor. As the name suggests, BLDC motor does not have brushes for commutation, but electronic commutation of stator windings is based on rotor position with respect to the stator windings. The Brushless Direct Current (BLDC) motor is widely used in many industrial applications, automotive, instrumentation, etc., due to its several advantages like better speed vs. torque characteristics, high dynamic response in transient states, high efficiency than conventional motor drives, long operation life irrespective of working conditions, noiseless operation over high-speed operations, higher speed ranges and easy controls [1]. Also, the torque delivered with respect to the size of the motor is higher, making it useful in applications where space and weight are critical factors like electric vehicles [2]. Torque of the BLDC motor is controlled by the waveform of back-EMF (the voltage induced into the stator winding due to rotor movement). Generally, the BLDC motors have trapezoidal back-EMF waveforms and are fed with rectangular stator currents, which give a theoretically constant torque. But, in practice, torque ripple exists, mainly due to back-EMF waveform imperfections, current ripple and phase current commutation. The current ripple result is from PWM generation technique or hysteresis control. The back-EMF waveform imperfections result from variations in the shapes of slot, skew and magnet of BLDC motor and are dependent on designing methods. An error can occur between actual value and the simulation results. Several simulation models have been proposed for the analysis of BLDC motor [3–6]. But simultaneously, two controls can be carried out to have smooth control over speed of motor. Inverter triggering is controlled by PWM generated by comparing the actual speed of rotor and the rotor position, and same rotor speed can be used to control speed of motor using controlled voltage source. In this paper, using this method PMBLDC motor speed is controlled and compared with the system uses inverter triggering using SPWM.

2 Mathematical Model

The BLDC motor is working as same as the traditional DC motor, but it is construction wise different from it. It is a self-rotating synchronous machine whose stator is similar to that of an induction motor, and the rotor has permanent magnet which is rotating part.

The circuit model of BLDC is as shown in Fig. 1, and the voltage equations of BLDC motor is given as:

$$V_a = R_a i_a + \frac{\mathrm{d}}{\mathrm{d}t}(L_{aa} i_a + L_{ab} i_b + L_{ac} i_c) + \frac{\mathrm{d}\lambda_{ar}(\theta)}{\mathrm{d}t}$$

Fig. 1 Motor circuit model

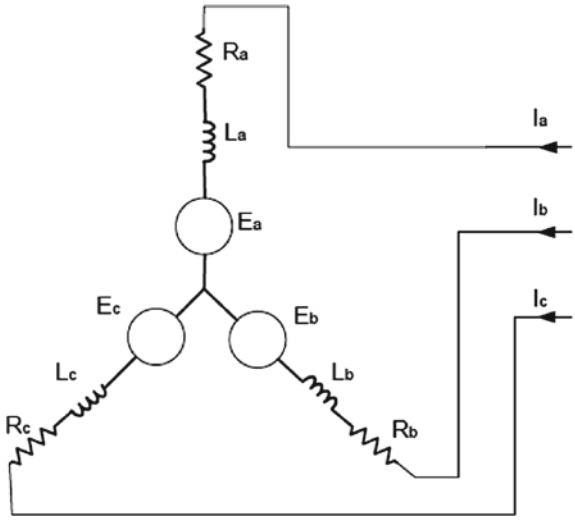

$$V_b = R_b i_b + \frac{\mathrm{d}}{\mathrm{d}t}(L_{ba} i_a + L_{bb} i_b + L_{bc} i_c) + \frac{\mathrm{d}\lambda_{br}(\theta)}{\mathrm{d}t}$$
$$V_c = R_c i_c + \frac{\mathrm{d}}{\mathrm{d}t}(L_{ca} i_a + L_{cb} i_b + L_{cc} i_c) + \frac{\mathrm{d}\lambda_{cr}(\theta)}{\mathrm{d}t}$$

Let us assume magnets have high sensitivity, all stator resistances are equal and rotor induced currents are neglected, then in matrix form for balanced system we have:

$$\begin{pmatrix} V_a \\ V_b \\ V_c \end{pmatrix} = \begin{pmatrix} R & 0 & 0 \\ 0 & R & 0 \\ 0 & 0 & R \end{pmatrix} \begin{pmatrix} i_a \\ i_b \\ i_c \end{pmatrix} + \frac{d}{dt} \begin{pmatrix} L_a & L_{ba} & L_{ca} \\ L_{ba} & L_b & L_{cb} \\ L_{ca} & L_{cb} & L_c \end{pmatrix} \begin{pmatrix} i_a \\ i_b \\ i_c \end{pmatrix} + \begin{pmatrix} e_a \\ e_b \\ e_c \end{pmatrix}$$

The above equations described the mathematical model of motor; hence, the rotor reluctance does not change with angle.

If,

$$L_a = L_b = L_{c|} = L$$

That is self and mutual inductance is constant, then the voltage equations become

$$\begin{pmatrix} V_a \\ V_b \\ V_c \end{pmatrix} = \begin{pmatrix} R & 0 & 0 \\ 0 & R & 0 \\ 0 & 0 & R \end{pmatrix} \begin{pmatrix} i_a \\ i_b \\ i_c \end{pmatrix} + \begin{pmatrix} L-M & 0 & 0 \\ 0 & L-M & 0 \\ 0 & 0 & L-M \end{pmatrix} \frac{\mathrm{d}}{\mathrm{d}t} \begin{pmatrix} i_a \\ i_b \\ i_c \end{pmatrix} + \begin{pmatrix} e_a \\ e_b \\ e_c \end{pmatrix}$$

And the electrostatic torque is given as:

$$T_e = \frac{e_a i_a + e_b i_b + e_c i_c}{w_r}$$

where *wr* is rotor speed (rad/sec).

Then equation of motion will be:

$$\frac{\mathrm{d}w_r}{\mathrm{d}t} = (T_e - T_l - Bw_r)/J$$

where B is friction constant (N-m/rad), Tl is load torque (N-m) and J is inertia of rotor and couple shaft (kg-m^2).

3 Method of Control

3.1 Rotor Speed and Rotor Position PWM

The schematic diagram of system is shown in Fig. 2, and MATLAB model is shown in Fig. 3. Two control loops are used; the inner loop synchronizes the inverter gate signals with the actual speed of rotor. The outer loop controls the motor's speed by varying the DC bus voltage using PI controller.

The gates signals for MOSFET-based inverter are derived from the error signal generated by comparing rotor actual speed and position of rotor sensed by Hall sensor which is decoded. Three-phase windings use one Hall sensors each, which are provided three overlapping signals giving a 60o wide position range. Whenever

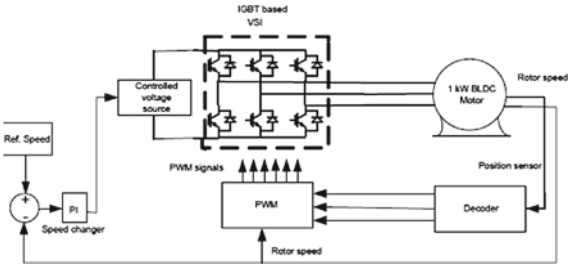

Fig. 2 Schematic diagram of system

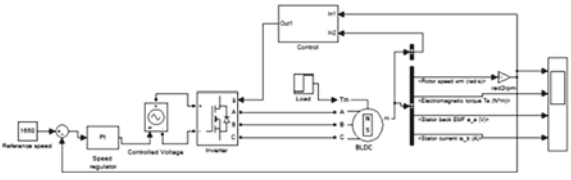

Fig. 3 MATLAB model of system

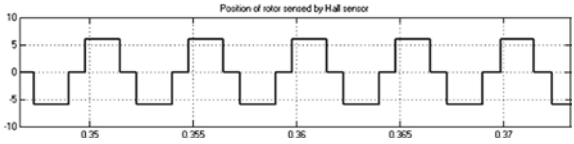

Fig. 4 Position of rotor decoded

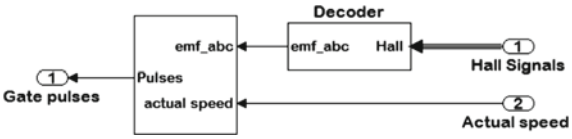

Fig. 5 Gate pulse control

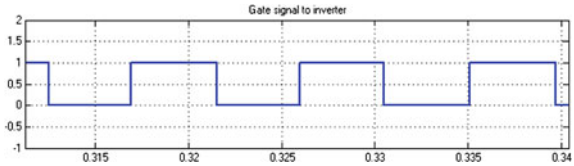

Fig. 6 Gate pulse to inverter

the magnetic poles pass near the sensors, they give high or low signal showing South and North Pole as shown in Fig. 4.

By varying the voltage across the motor terminals, we can control the speed of the BLDC, and when pulse is fed to six switches of the three-phase bridge, variation of motor voltage can be obtained by varying the duty cycle of the PWM signals. Inner closed-loop control is seemingly automatic as the position of rotor and speed of rotor are resulting due to rotation of rotor; hence, the gate signals to inverter will try to switch inverter in such a way to control the voltage input to motor, which will be corresponding to speed and position of rotor. The final speed control is fully done by outer closed loop, which is with speed changer or reference speed.

This method is more suitable for speed control for electric bike where the speed of wheel is in full control of throttle (Fig. 5).

The required speed is controlled by a speed controller. This is achieved by implementing conventional proportional-integral (PI) controller. PI was input by the difference in actual rotor speed and required speed. Based on this data, PI controller controls the duty cycle of PWM pulses which correspond to the voltage amplitude required to maintain the desired speed. Figure 6 shows the PWM pulses of 50% duty cycle.

3.2 Sinusoidal Pulse Width Modulation

Second method used is SPWM technique, where carrier wave is taken as triangular with variable frequency, and modulating wave is taken as decoded signal of rotor position sense by Hall sensor. The PWM generated by comparing these two waves

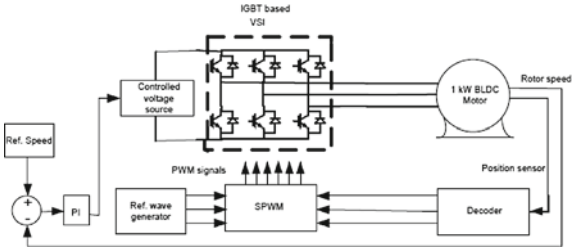

Fig. 7 Schematic diagram of SPWM technique

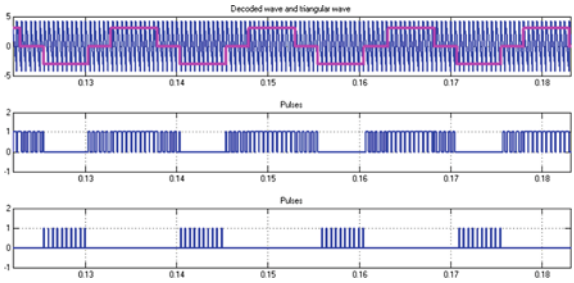

Fig. 8 Pulses of SPWM technique

is fed to inverter, as shown in Fig. 8. Figure 7 shows the schematic diagram of this technique.

4 Results and Discussions

A three-phase motor rated 1 kW, 500 Vdc, 3000 rpm is fed by a six step voltage inverter. The inverter is realized by MOSFET bridge. The three-phase output of the inverter is applied to the PMBLDC motor's stator windings. Load torque of 6 N-m is applied to the machine's shaft at $t = 0.5$ s, and differences are observed.

Figures 9 and 10 show the motor speed when required speed is set to 3000 rpm, and load torque of 9 N m is applied at $t = 0.5$ s, the differences in smoothness are clearly seen

The motor is tested further on different speed requirement such as 2500 rpm and 1650 rpm, and results are shown in Figs. 11, 12, 13and 14.

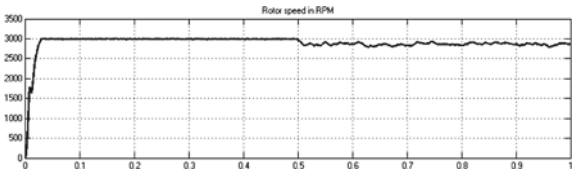

Fig. 9 Motor speed using RSRPPWM technique

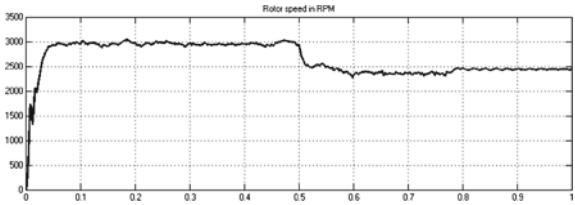

Fig. 10 Motor speed using SPWM technique

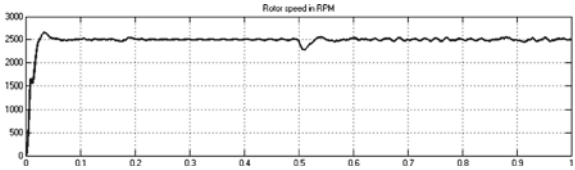

Fig. 11 Rotor speed with 2500 rpm using RSRPPWM technique

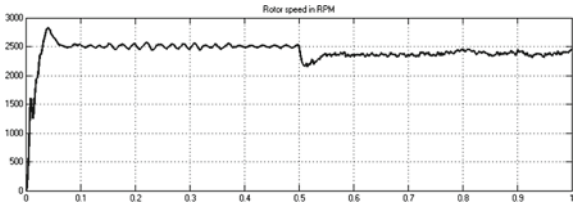

Fig. 12 Rotor speed with 2500 rpm using SPWM technique

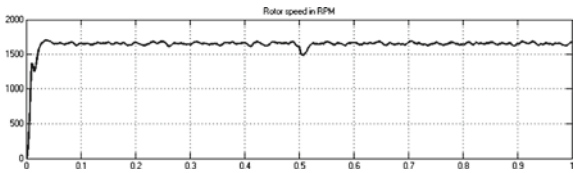

Fig. 13 Rotor speed with 1650 rpm using RSRPPWM technique

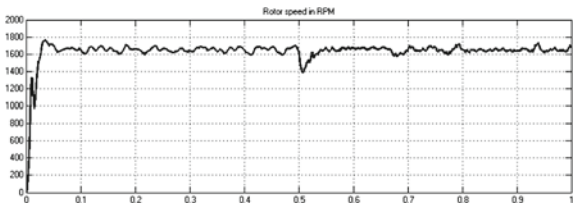

Fig. 14 Rotor speed with 1650 rpm using SPWM technique

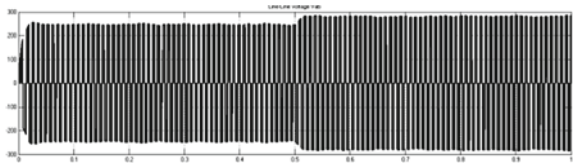

Fig. 15 Line-Line voltage to motor terminal

Figure 15 shows the line-to-line voltage applied to BLDC motor, which follows the desired pattern before load and after load application.

The time courses in Fig. 16a belong to the BLDC motor with trapezoidal back-EMF, and the responses are valid for sinusoidal back-EMF BLDC motor. There is very good correlation with the responses of the BLDC motor models known in references [7, 8] (Figs. 17, 18 and 19).

At closer look at the line-to-line voltage applied to motor reveals that the waveform is displaced by 120o, and it is quasi sinusoidal in shape.

The reference speed changing will alter the voltage applied to motor and thereby the speed of motor, especially in the application of motor for electric bike the robust control is demanded. The system is also tested on the variable required speeds and the correlation of required speed and rotor actual speed is studied, as shown in Figs. 20 and 21. It can be seen that using RSRPPWM technique has superior control over rotor speed, which is must need for electric bikes and other automobiles requiring fast and robust control. In Fig. 20, the differences in the higher speed between required and actual speed are because of rotors and coupler inertia (Figs. 22 and 23).

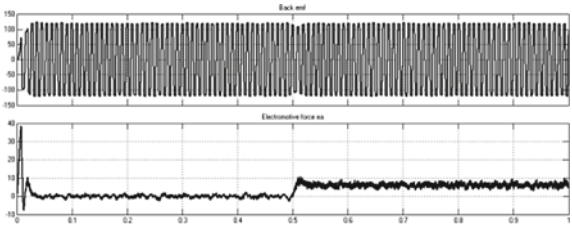

Fig. 16 Back-EMF and electromagnetic torque

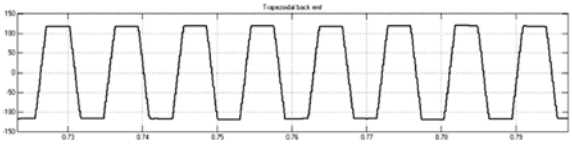

Fig. 17 Trapezoidal back-EMF

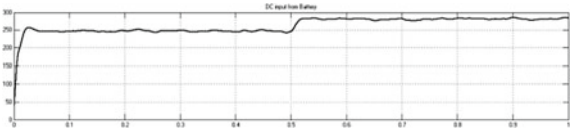

Fig. 18 DC input from battery

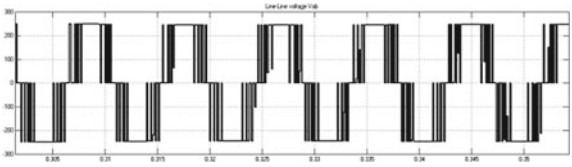

Fig. 19 Close look to voltage applied to motor

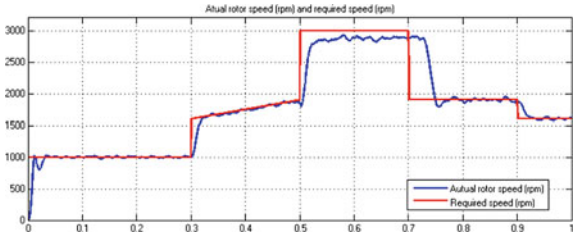

Fig. 20 Actual rotor speed and required speed using RSRPPWM technique

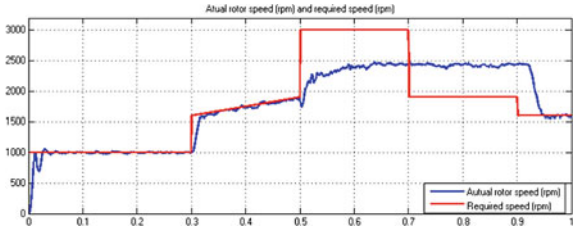

Fig. 21 Actual rotor speed and required speed using SPWM technique

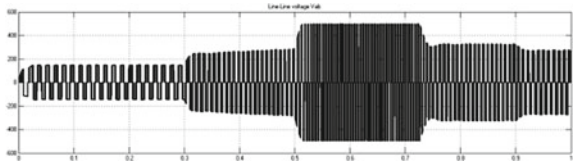

Fig. 22 Variation of motor input terminal voltages using RSRPPWM technique

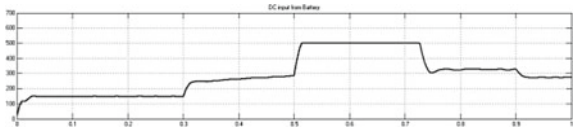

Fig. 23 Variation of DC input from battery using RSRPPWM technique

It is observed that using RSRPPWM technique is the best suited for controlling the speed of BLDC motor in automobile applications. The pulses to inverter will decide the motor speed and in turn, the speed of rotor will decide the pulse; hence, the technique of PWM generation performs vital role here. Figure 21 illustrates the out of relation of actual speed of rotor with required one, in between $t = 0.5$ s and $t = 0.9$ s the rotor speed literally constant without responding to required speed sent through speed changer. And at $t = 0.9$ s the rotor responded lately to the requirement of $t = 0.7$ s by speed changer. Also as shown in Fig. 21, at higher speed there exist large gap between two, which could be because of improper pulses.

5 Conclusion

Simulation and test run of proposed technique is done and presented, and it is seen that BLDC motor speed can effectively control by RSRPPWM technique. The performance results have shown that such method is very useful for applications requiring single outer closed-loop control. The results are at par with the theoretical predictions. The simulation result shows satisfactory performance and hardware implementation can be done. Further, the required speed input can be scaled down to 1 to 10 so that controlling becomes easier.

References

1. Civilian, R., & Stupak, D. (1995). Disk drive employing multi-mode spindle drive system. *U. S. patent 5471353*, Oct 3.
2. Jang, G. H., & Kim, M. G. (2005). A bipolar-starting and unipolar-running method to drive an HDD spindle motor at high speed with large starting. *IEEE Transactions on Magnetics, 41*(2), 750–755.
3. Kim, T. H., & Ehsani, M. (2003). An error analysis of the sensorless position estimation for BLDC motors 3. In *IEEE Conference of Industry Applications Conference, 38th IAS Annual Meeting* (Vol.1, pp. 611–617).
4. Hui, T. S., et al. (2003). Permanent Magnet Brushless motor control techniques. In *National Power and Energy Conference (PECon) 2003 Proceeding.* Bangi Malaysia.
5. Bianchi, N., et al. (2006). Comparison of PM motor structure and sensor less control techniques for zero-speed rotor position detection. *IEEE Transaction on Power Electronics, 22*(6), 2466–2475.
6. Thirusakthimurungan, P., et al. (2006). *A new control scheme for the speed control of MBLDC motor drive.* IEEE
7. Baldursson, S. (2005). *BLDC Motor Modelling and control-A MATLAB/Simulink Implementation (Master Thesis).*
8. Hong, W., Lee, W., & Lee, B. K. (2007). Dynamic simulation of brushless DC motor drives considering phase commutation for automotive application. In *IEEE International Electric machines and drives conferences* 2007 (pp 1377–1383). IEMDC 3–5 May 2007.
9. Kotrba, A., Yetkin, A., Gough, B., Gundogan, A., Mastbergen, D, & Paterson, C. (2011). *Performance characterization of a thermal regeneration unit for exhaust*. Presented at the Commercial Vehicle Engineering Congress, Rosemont, IL, USA, Paper SAE 2011-01-2208.
10. Song, J.-H., & Choy, I. (2004). Commutation torque ripple reduction in brushless DC motor drives using a single DC current sensor. *IEEE Transactions on Power Electronics, 19*(2), 312–319.
11. Tsai, M.-F., PhuQuy, T., Wu, B.-F., & Tseng, C.-S. (2011). Model construction and verification of a BLDC motor using MATLAB/SIMULINK and FPGA control. In *Proceedings 6th IEEE Conference Industrial Electronic Application* (pp. 1797–1802). Beijing.